The Wuhan Atmospheric Radio Exploration (WARE) Radar: Implementation and Initial Results

Chen Zhou*, Haiyin Qing, Gang Chen, Xudong Gu, Binbin Ni, Guobin Yang, Yuannong Zhang, Zhengyu Zhao

Ionosphere Laboratory, School of Electronic Information,

Wuhan University, Wuhan, Hubei 430072, China

* Correspondence to: Chen Zhou (chen.zhou.whu@gmail.com)

Abstract

The recently constructed Wuhan Atmospheric Radio Exploration (WARE) radar is the first mesosphere-stratosphere-troposphere (MST) radar in the mainland of China, located at Chongyang, Hubei Province (114°8'8”E, 29°31'58”N, ~ 23° geomagnetic latitude). WARE radar has a capability of probing the structure and dynamics of the atmosphere at the altitudes from 3 km to 100 km (excluding 25 km – 60 km). With fine temporal and spatial resolution, WARE radar provides an outstanding opportunity ~~for the first time~~ to extensively and intensively investigate various atmospheric phenomena at the regions of mid-latitude China. In this paper, we present the main configuration and technical specifications of WARE radar system. For the first time, we report some initial results: (1) wind field observation from 69 km to 85 km, and wind field observation from 3.2 km to 16.9 km with comparison with results

of rawinsonde; (2) tropopause height determined by radar echo power and comparison between radar tropopause and rawinsonde tropopause (3) atmospheric gravity waves in the troposphere with ~~wave length~~wavelength and propagation direction analyzed by hodograph method; (4) aspect sensitivity of echo power at six specified heights in the troposphere and stratosphere; (5) diurnal and semi-diurnal tides in tropospheric and low stratospheric height analyzed by Lomb-Scargle periodogram method.

1 Introduction

In the past 30 years, mesosphere-stratosphere-troposphere (MST) radars have been developed and installed around the world. MST radar observes the echoes backscattered from refractive index fluctuations in the neutral atmosphere and ionosphere, which can be applied to operational routine observation and scientific research. The first Very-high-frequency (VHF) MST radar in Jicamaca successfully observed the atmospheric echoes in 1970s (Woodman and Guillen, 1974). Since then, studies and constructions of MST radars have shown great growth. For example, the SOUSY radars (Czechowsky et al., 1984; Rüster et al., 1986), the Esrange radar (Clison et al., 1999) and the recent MARRSY MST radar (Latteck et al., 2012) in Norway have shown great capacities for atmospheric research in Europe. VHF MST radars have also developed widely in the Unite States since 1970s (Gage and Balsley, 1978; Gage and Green, 1978; Hocking et al., 2001). In Asia, there have been several VHF-MST radars, such as the middle and upper atmosphere (MU) radar (Fukao et al., 1980, 1990), the Chung_Li radar (Röttger et al., 1990), the Gadanki radar (Rao et al., 1995; ~~Jein~~Jain et al., 1995), the Equatorial Atmosphere Radar (EAR) radar (Fukao et al., 2003), and so on, which have provided numerous important results and findings to further our understandings of the atmosphere and the ionosphere.

Enormous progresses have been made into the atmospheric research by VHF-MST radars (see the reviews by Hocking (1997; 2001), Fukao (2007) and the references therein). One of the most important purposes of MST radars is routinely continuous monitoring the three-dimensional atmospheric winds at altitudes above the boundary layer. Doppler Beam Swinging (DBS) and Spaced Antenna (SA) methods are the two primary methods for deriving wind field estimation of MST radars. In particular, MST radars is capable of measuring the profiles of vertical wind velocities. Conventionally, the tropopause height is determined from atmospheric temperature by rawinsonde observations. MST radars provide an effective and efficient approach to estimate the detailed temporal variation of tropopause, which is very important for studies of atmospheric dynamics. Due to the fine temporal resolution of three dimensional wind measurement at different height, MST radars are the most suitable instruments for atmospheric gravity waves (AGWs) studies, including intrinsic frequencies, wavelengths, wavenumber spectra, and possible wave sources. Studies of aspect sensitivity of echo power have always been a significant topic for MST radar community. For MST research, aspect sensitivity means angle dependence of echo power, which can be employed to investigate the primary mechanism (scattering or reflection) of the MST radar echoes. With the fine temporal resolution, MST radar is also suitable for tidal analysis and nonlinear coupling between different atmospheric waves and oscillations such as AGWs, planetary waves (PW), and quasi biennial oscillation (QBO).

Although considerable development of technology and applications for MST studies have been made, new instruments and facilities are still planned and proceeded for further atmospheric research. Recently, Wuhan Atmospheric Radio Exploration (WARE; 114°8'8”E, 29°31'58”N) radar has been successfully developed and put into operation (Zhao et al., 2013). The WARE radar is a significant facility of the Meridian Space Weather Monitoring Project of China (Wang, 2010) that conduct a comprehensive multi-layered and inter-disciplinary survey and exploration of space environment by advanced ground based techniques. The WARE radar has great potential to yield new findings, especially for regional atmospheric characteristics, due to the capabilities for comprehensive atmospheric research.

In this report the design and the implementation of WARE radar system is summarized. For the first time we present a number of initial observations of WARE radar, including measurements of tropospheric and mesospheric wind, determination of the tropopause, studies of AGWs, tropospheric aspect sensitivity and atmospheric tides investigation.

2 Brief Description of WARE Radar System

The WARE radar is the first MST radar put into service in mainland of China, which is located at Chongyang, Hubei Province of China (114°8'8"E, 29°31'58"N) with the geomagnetic latitude of ~ 23°. The altitude of the radar site is 62 meters above the sea level. The inclination and declination angles of geomagnetic field are approximately 44.7° and -3.7° respectively at the altitude of 110 km above the radar site.

The WARE radar is a fully distributed, all solid state, and coherent pulsed Doppler radar operating at 53.8 MHz with an average power aperture product of 2.3×10^8 Wm^2. The reliable detection height range covers from roughly 3 km to 100 km (not including 25 km – 60 km). The phased array of WARE radar consists of 24×24 three-element Yagi-Uda antennas evenly distributed over a total area of 10000 m^2. The radar beam can be steered into five directions (East, West, South, North, and vertical) independently, changing continuously from vertical to 20° off-zenith angle with a step of 1° from pulse to pulse. The echoes from five beams are collected alternately by the receiver. DBS and active phased array technique are utilized to probe the structure and the dynamics of the atmosphere. WARE radar is designed to operate at three independent modes which correspond to monitoring the troposphere (low mode, 3.5 km – 10 km), the low stratosphere (medium mode 10 km – 35 km), and the mesosphere (high mode 60 km – 90 km), respectively.

Characteristics of atmospheric turbulence echoes, including the Doppler velocity and spectrum width, are estimated after removal of background noise and clutter. Distinct from time domain pulse radar system, clutter suppression is accomplished by spectrum analysis due to frequency domain detection of WARE radar. The technical parameters and performance parameters of three modes are tabulated in Table 1, respectively. More detailed description about WARE system and hardware can be found in Zhao et al. (2013).

3 Preliminary Results of WARE Radar Observations

3.1 Observations of atmospheric wind field

Measurement of fine quality wind field is one of the major objectives of MST radars~~ (Gage and Vanzandt, 1981; Balsley, 1983)~~. WARE radar has the capability of measuring the wind field based upon the DBS technique. Comparisons of wind field observations between WARE radar and GPS rawinsonde were carried out immediately after the WARE radar was established. Figure 1 (a) presents the power spectrum of radar echoes received by the east, west, south, and north beams tilted to 20° off-zenith angle, and Figure 1 (b) shows the comparison of radar wind and rawinsonde wind obtained at 16:00 LT on September 11, 2011. Clearly, the observations of WARE radar are reasonably consistent with the rawinsonde observations for both wind velocity and wind direction, indicating that our newly constructed WARE radar works properly and efficiently to provide reliable observations for further studies. One of the potential capability of MST radar is to provide the direct wind measurement of vertical velocity. Figure 2 presents vertical velocity for continuous 24 hours on October 2, 2012.

An example of mesospheric wind field measurements from 69 to 85 km obtained by WARE radar on March 15, 2011 is shown in Figure ~~2~~3. Figure ~~2~~ 3 (a) presents the power spectrum received by east, west, south, and north beams tilted to 20 °off-zenith angle. Up to 20 ° off-zenith beams are utilized for the mesospheric wind estimation, which cover a vast horizontal area and get enough horizontal wind velocity component. However, these measurement need more homogenous backscatter in the observation volume (Browing and Wexler 1967; Waldteufel and Corbin 1973; Stober et al., 2013).

Figure ~~2~~ 3 (b) presents the meridional and zonal wind estimated by echo power spectrum. Lee et al. (2014) suggest an influence from local mountain waves. The WARE radar is located at the Jianghan Plain, no large mountain ridges are close to the radar site. Small uncontinuous foothills are located about 50 km south of the radar, which could produce mountain lee waves. These potential waves could induce uncertainties in radar wind measurement. (Stober et al., 2011)

~~–~~It is expected that the long-term observation by WARE radar will establish a unique database to investigate the profiles of mesospheric wind in the mid-latitude region of China.

3.2 Observations of the tropopause

Tropopause is a natural stable layer which plays a significant role in the stratosphere-troposphere exchange (STE). Characteristics of tropopause have been studied in many ways and in many regions (Reid and Gage, 1996; Hermawan et al., 1998; Yamamoto et al., 2003; Das et al., 2008; Mehta et al., 2008, 2011). The detailed time variation of tropopause structure is very important for studies of dynamical atmospheric properties. WARE radar provides a good opportunity to study the mid-latitude tropopause.

Conventionally, the height of tropopause can be determined by the lapse rate (lapse rate tropopause, LRT) (World Meteorological Organization (WMO), 1996), cold point (cold point tropopause, CPT) (Selkirk, 1993), and radar echo power (radar tropopause, RT) (Gage and Green, 1979, 1982; Hall et al., 2009). In our present study, we simply adopt refractivity structure constant (C_n^2) derived from radar echo power to evaluate the tropopause location (Rao et al., 1997; Ghosh et al., 2001; Zink et al., 2004). Two experiments are shown in Figure 3(a), which were executed around 17:15 LT on September 10, 2011 and around 07:21 LT on September 11, 2011 for validation of the radar measurements. The green line in Figure 3(a) is the C_n^2 value estimated from radar echo power. The location of maximum C_n^2 value implies the height of tropopause, which was about 16 km in the two cases. The blue points are the recorded temperature derived from rawinsonde and the blue line is the fitted temperature profile. The coldest point of the temperature is the height of tropopause determined by rawinsonde, which was about 17 km. The location of tropopause can be different according to different tropopause definitions and tropopause dynamics. (Yamamoto et al., 2003; Das et al., 2008) In addition, the tropopause is not just a thin layer but a transition region between the troposphere and stratosphere (Mehta et al., 2008). Figure 4 (a) demonstrate the difference between the cold point tropopause (CPT) from rawinsonde and radar tropopause. It should also be noted that the height resolution is 0.6 km in the medium operational mode, which add some uncertainties for radar tropopause location. ~~Considering that the height resolution of WARE radar operated at medium mode is 0.6 km, the heights of tropopause derived from radar and rawinsonde are consistent with each other basically.~~

After validation of radar tropopause, a 20.5-hour observation was carried out from 08:05 LT, January 2, 2012 to 04:35 LT, January 3, 2012. Figure ~~3~~ 4 (b) shows the result. As seen, the height of radar tropopause was between 11 km to 12 km during this time period, which was much lower than that 1 shown in Fig. ~~3~~ 4 (a). Variation in tropopause height can be attributed to different seasons for the radar observations. The tropopause height is usually higher in summertime than in wintertime.

3.3 Observations of atmospheric gravity waves

Atmospheric gravity waves (AGWs) play an important role in transporting energy and momentum, in contributing turbulence and mixing, and in influencing the mean circulation and thermal structure of the middle atmosphere (Fritts and Alexander, 2003). In addition, AGWs are crucial to understand the coupling process of the upper atmosphere and the ionosphere (Hines, 1960). Quasi-monochromatic (QM) AGWs are frequently observed with airglow imagers, lidars, radars and rawinsondes. On this aspect, WARE radar provides a standard and effective tool to study these AGWs. Hodograph method (Gavrilov et al., 1996; 1997; Hu et al., 2002; Zhang and Yi, 2005) is utilized here to extract the parameters of dominant QM AGWs. To obtain the parameters of AGW, the background winds are firstly removed by fitting a second order polynomial to the horizontal wind profiles (Zhang and Yi, 2005). The results shown in Figure 4 are two typical examples of QM AGWs observed by WARE radar at 06:05 LT and 13:05 LT, on September 26, 2011. Figure ~~4~~ 5 (a) and (b) show wave fits of vertical profiles of meridional wind disturbance at heights from 3.04 to 9.85 km at two respective scenarios, while Figure ~~4~~ 5 (c) and (d) show the zonal component. Figure ~~4~~ 5 (e) and (f) present the vertical wind disturbance. The wavelenght~~wave lengths~~ of the two QM AGWs are calculated to be 4.99 km and 3.25 km, respectively. Hodographs of the meridional wind versus zonal wind are illustrated in Figure ~~4~~ 5 (g) and (h). The rotations are both anti-clockwise, indicating downward propagating waves.

By analyzing the polarization relation of AGW, the AGW horizontal propagation directions are parallel to the major axis of the ellipse in hodographs. We can estimate the propagation directions are 23° or 23°+180° and 45° or 45°+180°, since the directions have 180° ambiguity. In order to resolve this ambiguity, the simultaneous measurement of the temperature profile can be utilized by radiosonde observations or

Na lidar (Hu et al., 2002; Zhang and Yi, 2005), However WARE radar can not provide the temperature profile directly, the ambiguity can also be eliminated by the vertical wind profile (Muraoka et al., 1987; Tsuda et al., 1990). Hence the horizontal propagation direction can be determined by combination of the hodograph method and the measurement of vertical velocity of wind. For the cases presented in Figure 4, the horizontal propagation directions are finally identified as 23° (left column) and 225° (right column), which are clockwise to the north. The wave intrinsic frequencies of these QM AGWs are also calculated according to the hodographs, which is 10.3 hour and 7.2 hour, the local Coriolis frequency is 7.29×10^{-5} rads^{-1}. These QM AGWs in the upper troposphere have been frequently observed by WARE radar, a statistical analysis of which is our undertaking work.

3.4 Observations of aspect sensitivity of echo power

Aspect sensitivity means the dependence of echo power on antenna beam pointing angle, which has been reported by several researchers (Gage and Green, 1978; Röttger and Liu, 1978; Tsuda et al., 1986). MST radar echoes are known to be aspect sensitive due to anisotropic backscattering and Fresnel reflection/scattering, which in turn influence the determination of wind components and measurement of turbulence parameters. Jain et al. (1997) suggested that for smaller beam angles the horizontal wind component may be underestimated by as much as 30%. Therefore several theoretical models are proposed to explain scattering/reflection mechanisms in order to facilitate the understanding of aspect sensitivity and its effect on the radar echoes.

WARE radar operates at five beams including one vertical beam and four oblique beams. Each oblique beam has been designed to be able to scan from vertical to 20° continuously with a step of 1°. Therefore WARE radar has the capability for investigating the zenith angle dependence of the backscattered echo power at different altitudes. Figure ~~5~~ 6 shows the variation of echo power as a function of beam zenith angle at six specified heights from 4.75 km to 17.85 km. Observations are carried out at 13:13 LT, December 27, 2011.

Figure ~~5~~ 6 shows that (1) aspect sensitivity occurs throughout the troposphere and low stratosphere; (2) aspect sensitivity is higher in the troposphere than in the stratosphere in this observation; (3) the relative echo power for smaller zenith angles ($\leq 10°$) decreases faster than the larger angles ($>10°$). Usually, the degree of aspect sensitivity is lower in the troposphere than in the stratosphere. This is due to turbulent air in the troposphere and stable atmosphere in the stratosphere. There are several interpretations on the causative mechanisms of aspect sensitivity. Fresnel reflection/scattering and anisotropic scattering are the two leading suggestions. (Röttger and Liu, 1978; Crane, 1980; Doviak and Zrnic, 1984; Woodman and Chu, 1989) Study of aspect sensitivity can yield a deeper understanding of the mechanisms of the atmospheric radar echoes, like isotropic/anisotropic turbulence or Fresnel reflecting/scattering structures. However, it is difficult to separate the respective contributions of these echoing mechanisms. In this case, we present irregular pattern of aspect sensitivity at six specified heights of troposphere and low stratosphere, which could be an evidence for the complicated interpretation of atmospheric aspect sensitivity and that combined mechanism could make contributions. Radar echoes also could be come from different scatters, especially at low beam angles (Chen and Furumoto, 2013). Tsuda et al. (1997) suggest that horizontal component of atmospheric gravity wave motions could distort the refractivity surface. This mechanism could also generate irregular pattern of aspect sensitivity.~~Our observation indicate that the mechanism for aspect sensitivity could be complicated and Different interpretations should be taken into consideration.~~

3.5 Observations of diurnal and semi-diurnal tides

Atmospheric tides are defined as atmospheric waves or oscillations with periods of harmonics of a solar day. The subset migrating tides propagate westward with zonal wavenumbers equal to the frequencies in cycles per day. The migrating tides are generated primarily by ozone heating in the stratosphere and water vapor heating in the troposphere, which are uniform zonal distributed. The zonal wavenumbers of nonmigrating tides are not equal to the frequencies in cycles per day, which have more local characteristics. Tides are believed to play an important role in large scale circulation patterns and the dynamics of mesosphere and lower thermosphere. (Forbes, 1982; Forbes et al., 1997; Vincent et al., 1998; Manson et al., 2002) However, due to the small amplitudes of tides in the troposphere and lower stratosphere, the studies on tides in this region require more efforts and deserve further investigation.

We report diurnal and semi-diurnal tide analysis by WARE radar observations in the lower atmosphere from October 1 to October 12, 2011. The observations of WARE radar provide 30 minutes time resolution and allow us to analyze in the temporal domain. Meridional and zonal wind are firstly derived from power spectrum of radar echoes. Figure ~~6~~ 7 (a) and Figure ~~7~~ 8 (a) show meridional and zonal wind from 3 km to 25 km with height resolution of 150 meters during continuous 12 days. Then the perturbation wind field is obtained by subtracting the background wind. We calculate the background wind by applying a second-order polynomial fitting to the vertical profiles of horizontal and vertical winds respectively, following Zhang and Yi (2005). After that, a high pass filter with a cutoff at 36 h is applied to remove the influence of planetary waves (PW) and quasi biennial oscillation (QBO). Finally, a Lomb-Scargle periodogram analysis (Scargle, 1981; 1982) is performed on the resultant time series data. Significant values in Figure ~~6~~ 7 (b) and Figure ~~7~~ 8 (b) can be found around the period of 12 hour and 24 hour, which indicate semi-diurnal and diurnal oscillation. It should also be noted that at the low altitude the values concentrate on the 12 hour and 24 hour, while at the high altitude the values tend be scattered around these two periods. The results indicate the influence of secondary waves generated by the planetary/tidal wave interaction. ~~(Huang et al., 2009)~~

Tidal horizontal wind amplitudes can reach to several tens of m/s in mesosphere and low thermosphere, which have been intensively studied for thirty years. However, due to the weak amplitude, tides in troposphere and lower stratosphere have not been subjected to sufficient study. Recent research with intense rawinsonde and radar measurement [Whiteman et al, 1996; Huang et al, 2009; Sakazaki et al, 2010] have presented tidal wind perturbations in tropospheric and low stratospheric data. However, due to nonlinear wave-flow and wave-wave interactions, tidal frequency spectral estimation could be biased with periods around the diurnal and semi-diurnal tides.

4. Summary

Here in this paper we have summarized the design and implementation of WARE radar – the first VHF-MST radar in the mainland of China. A number of initial results regarding atmospheric wind field, tropopause, atmospheric gravity waves (AGWs), aspect sensitivity of echo power, and atmospheric tides have been reported. These results demonstrate the outstanding capabilities of WARE radar for comprehensive atmospheric researches. We have a strong feeling that as a unique VHF-MST radar facility at mid-latitude in the mainland of China and as an integrated part of well-planned Chinese Meridian Space Weather Monitoring Project, WARE radar has great potentials to yield new findings especially of the regional atmospheric characteristics. Further system improvements and expansions will include radio acoustic sounding system (RASS) to obtain local temperature profiles. Combinations of AGWs observations by WARE radar with simultaneous GPS network and HF

Doppler observations is also able to provide profound clues to track the correlations between AGWs and TIDs. Therefore, this kind of study can greatly enhance our knowledge of the neutral atmosphere-ionosphere coupling process, especially at low- and middle-latitudes. Collaborative experiment campaigns of our WARE MST radar, for instance, during the deep convection, cold front, Mei-Yu season, and / or magnetic storms, together with the MU radar and the Chung-Li radar, all of which are located in East Asia, will establish a truly unique platform for in-depth investigations and comprehensive understandings of the structures and the dynamics of the Earth's atmosphere.

Acknowledgements

We thank Prof. Shaodong Zhang, Prof. Jingfang Wang, and Xiaoming Zhou for invaluable discussions and warm-hearted helps on many aspects. We also thank the fruitful collaborations of the colleagues and the staff of the Meridian Space Weather Monitoring Project of China. This work was supported by the National Natural Science Foundation of China (NSFC grant No. 41204111). CZ appreciate the support by Wuhan University "351 Talents Project". The data for this paper are available at Data Centre for Meridian Space Weather Monitoring Project (http://159.226.22.74/). The rawinsonde data can be provided by corresponding author via private communication.

Reference

Balsley, B. B., Ecklund, W. L., Carter, D. A., and Johnston, P. E.: The MST radar at Poker Flat, Alaska, Radio Sci., 15(2), 213–223, doi:10.1029/RS015i002p00213, 1980.

~~Balsley, B. B.: Poker Flat MST radar measurement of winds and wind variability in the mesosphere, stratosphere, and troposphere, Radio Sci., 18(6), 1011–1020, doi:10.1029/RS018i006p01011, 1983.~~

Browning, K. and Wexler, R.: The Determination of Kinematic Properties of a Wind field Using Doppler Radar, J. Appl. Meteorol., 7, 105–113, 1968.

Chen, Jenn-Shyong and Furumoto, Jun-ichi: Measurement of Atmospheric Aspect Sensitivity Using Coherent Radar Imaging after Mitigation of Radar Beam Weighting Effect. J. Atmos. Oceanic Technol., 30, 245–259, 2013.

Chilson, P. B., Kirkwood, S., and Nilsson, A.: The Esrange MST radar: A brief introduction and procedure for range validation using balloons, Radio Sci., 34(2), 427–436, doi:10.1029/1998RS900023, 1998.

Chu, Y. H., Chao, J. K., Liu, C. H., and Röttger, J.: Aspect sensitivity at tropospheric heights measured with vertically pointed beam of the Chung-Li VHF radar, Radio Sci., 25(4), 539–550, doi:10.1029/RS025i004p00539, 1990.

Crane, R. K.: A review of radar observations of turbulence in the lower stratosphere, Radio Sci., 15(2), 177–193, doi:10.1029/RS015i002p00177, 1980.

Czechowsky, P., Schmidt, G., and Rüster, R.: The mobile SOUSY Doppler radar:

Technical design and first results, Radio Sci., 19(1), 441–450, doi:10.1029/RS019i001p00441, 1984.

Das, S. S., Jain, A. R., Kumar, K. K., and Rao, Narayana D.: Diurnal variability of the tropical tropopause: Significance of VHF radar measurements, Radio Sci., 43, RS6003, doi:10.1029/2008RS003824, 2008.

Doviak, R. J., and Zrnic', D. S.: Reflection and scatter formula for anisotropically turbulent air, Radio Sci., 19(1), 325–336, doi:10.1029/RS019i001p00325, 1984.

Forbes, J. M.: Atmospheric tides: 1. Model description and results for the solar diurnal component, J. Geophys. Res., 87(A7), 5222–5240, doi:10.1029/JA087iA07p05222, 1982.

Forbes, J. M., Hagan, M. E., Zhang, X., and Hamilton, K.: Upper atmosphere tidal oscillations due to latent heat release in the tropical troposphere, Ann. Geophys., 15, 1165–1175, 1997.

Fukao, S., Kato, S., Aso, T., Sasada, M., and Makihira, T.: Middle and upper atmosphere radar (MUR) under design in Japan, Radio Sci., 15(2), 225–231, doi:10.1029/RS015i002p00225, 1980.

Fukao, S., Hashiguchi, H., Yamamoto, M., Tsuda, T., Nakamura, T., Yamamoto, M. K., Sato, T., Hagio, M., and Yabugaki, Y.: Equatorial Atmosphere Radar (EAR): System description and first results, Radio Sci., 38, 1053, doi:10.1029/2002RS002767, 3, 2003.

Fukao, S.: Recent Advances in Atmospheric Radar Study, J. Meteor. Soc. Japan, 85B, 215-239, 2007.

Fukao, S., Sato, T., Tsuda, T., Yamamoto, M., Yamanaka, M. D., and Kato, S.: MU radar: New capabilities and system calibrations, Radio Sci., 25(4), 477–485, doi:10.1029/RS025i004p00477, 1990.

Fritts, D. C., and Alexander, M. J.: Gravity wave dynamics and effects in the middle atmosphere, Rev. Geophys., 41(1), 1003, doi:10.1029/2001RG000106, 2003.

Gage, K. S., and Balsley, B. B.: Doppler radar probing of the clear atmosphere, Bull. Am. Meteorol. Soc., 59, 1074-1093, 1978.

Gage, K. S., and Green, J. L.: Evidence for specular reflection from monostatic VHF radar observations of the stratosphere, Radio Sci., 13(6), 991–1001, doi:10.1029/RS013i006p00991, 1978.

Gage, K. S., and Green, J. L.: Tropopause detection by partial specular reflection with very-high-frequency radar, Science, 203, 1238–1240, doi:10.1126/science.203.4386.1238, 1979.

~~Gage, K. S., and Vanzandt, T. E.: Wind Measurement Techniques Available for the Middle Atmosphere Program, J. Geophys. Res., 86(C10), 9591-9598, doi:10.1029/JC086iC10p09591, 1981.~~

Gage, K. S., and Green, J. L.: An objective method for the determination of tropopause height from VHF radar observations, J. Appl. Meteorol., 21, 1150–1154, 1982.

Gavrilov, N. M., Fukao, S., Nakamura, T., Tsuda, T., Yamanaka, M. D., and

Yamamoto, M.: Statistical analysis of gravity waves observed with the middle and upper atmosphere radar in the middle atmosphere: 1. Method and general characteristics, J. Geophys. Res., 101(D23), 29511–29521, doi:10.1029/96JD01447, 1996.

Gavrilov, N. M., Fukao, S., Nakamura, T., and Tsuda, T.: Statistical analysis of gravity waves observed with the middle and upper atmosphere radar in the middle atmosphere: 2. Waves propagated in different directions, J. Geophys. Res., 102(D12), 13433–13440, doi:10.1029/97JD00736, 1997.

Ghosh, A. K., V. Siva Kumar, K. Kishore Kumar, and A. R. Jain (2001), VHF radar observation of atmospheric winds, associated shears and C2n at a tropical location: interdependence and seasonal pattern, Ann. Geophys., 19, 965-973, doi:10.5194/angeo-19-965-2001, 2001.

Hall, C. M., Röttger, J., Kuyeng, K., Sigernes, F., Claes, S., and Chau, J.: First results of the refurbished SOUSY radar: Tropopause altitude climatology at 78 °N, 16 °E, 2008, Radio Sci., 44, RS5008, doi:10.1029/2009RS004144, 2009.

Hines, C. O.: Internal atmospheric gravity waves at ionospheric heights, Can. J. Phys., 38, 1441-1481, 1960.

Hocking, W. K., Rüster, R., and Chechowsky, P.: Absolute reflectivities and aspect sensitivities of VHF radio wave scatterers measured with the SOUSY radar, J. Atmos. Terr. Phys., 48, 131–144, 1986.

Hocking, W. K.: Recent advances in radar instrumentation and techniques for studies of the mesosphere, stratosphere, and troposphere, Radio Sci., 32(6), 2241–2270, 1997.

Hocking, W. K., Kelley, M., Rogers, R., Brown, W. O. J., Moorcroft, D., and St. Maurice, J.-P.: Resolute Bay VHF radar: A multipurpose tool for studies of tropospheric motions, middle atmosphere dynamics, meteor physics, and ionospheric physics, Radio Sci., 36(6), 1839–1857, doi:10.1029/2000RS001005, 2001.

Hocking, W. K.: A review of Mesosphere-Stratosphere-Troposphere (MST) radar developments and studies, circa 1997-2008, J. Atmos. Solar-Terr. Phys., 73(9), 848-882, doi:10.1016/j.jastp.2010.12.009, 2011.

Hu, X., Liu, A. Z., Gardner, C. S., and Swenson, G. R.: Characteristics of quasi-monochromatic gravity waves observed with Na lidar in the mesopause region at Starfire Optical Range, NM, Geophys. Res. Lett., 29(24), 2169, doi:10.1029/2002GL014975, 2002.

Huang, C. M., Zhang, S. D., and Yi, F.: Intensive radiosonde observations of the diurnal tide and planetary waves in the lower atmosphere over Yichang (111°18' E, 30°42' N), China, Ann. Geophys., 27, 1079-1095, doi:10.5194/angeo-27-1079-2009, 2009.

Jain, A. R., Rao, Y. Jaya, and Rao, P. B.: Aspect sensitivity of the received radar backscatter at VHF: Preliminary observations using the Indian MST radar, Radio Sci., 32(3), 1249–1260, doi:10.1029/97RS00252, 1997.

Jain, A. R., Rao, Y. J., Rao, P. B., Anandan, V. K., Damle, S. H., Balamuralidhar, P., Kulakarni, A., and Viswanathan, G.: Indian MST radar 2. First scientific results in ST mode, Radio Sci., 30(4), 1139–1158, doi:10.1029/95RS00652, 1995.

Latteck, R., Singer, W., Rapp, M., Vandepeer, B., Renkwitz, T., Zecha, M., and Stober, G.: MAARSY: The new MST radar on Andøya—System description and first results, Radio Sci., 47, RS1006, doi:10.1029/2011RS004775, 2012.

Manson, A. H., Luo, Y., and Meek, C.: Global distributions of diurnal and semi-diurnal tides: observations from HRDI-UARS of the MLT region, Ann. Geophys., 20, 1877–1890, 2002.

Mehta, S. K., Murthy, B. V. K., Rao, D. N., Ratnam, M. V., Parameswaran, K., Rajeev, K., Raju, C. S., and Rao, K. G.: Identification of tropical convective tropopause and its association with cold point tropopause, J. Geophys. Res., 113, D00B04, doi:10.1029/2007JD009625, 2008.

Mehta, S. K., Ratnama, M. V., and Murthyb, B. V. K.: Characteristics of the tropical tropopause over different longitudes, J. Atmos. Solar-Terr. Phys., 73(17-18), 2462-2473, doi:10.1016/j.jastp.2011.09.006, 2011.

Muraoka Y., Kawahira, Sato, K. T., Tsuda, T., Fukao, S., and Kato, S.: Characteristics of mesospheric internal gravity waves observed by MU Radar. Geophys. Res. Lett., 14(11), 1154–1157, doi: 10.1029/GL014i011p01154, 1987.

Rao, P. B., Jain, A. R., Kishore, P., Balamuralidhar, P., Damle, S. H., and Viswanathan, G.: Indian MST radar 1. System description and sample vector wind measurements in ST mode, Radio Sci., 30(4), 1125–1138, doi:10.1029/95RS00787, 1995.

Rao, D. N., Kishore, P., Rao, T. N., Rao, S. V. B., Reddy, K. K., Yarraiah, M., and Hareesh, M.: Studies on refractivity structure constant, eddy dissipation rate, and momentum flux at a tropical latitude, Radio Sci., 32(4), 1375–1389, doi:10.1029/97RS00251, 1997.

Reid, G. C., and Gage, K. S.: The tropical tropopause over the western Pacific: Wave driving, convection, and the annual cycle, J. Geophys. Res., 101(D16), 21,233–21,241, doi:10.1029/96JD01622, 1996.

Röttger, J., and Liu, C. H.: Partial reflection and scattering of VHF radar signals from the clear atmosphere. Geophys. Res. Lett., 5: 357–360. doi: 10.1029/GL005i005p00357, 1978

Röttger, J., et al.: The Chung-Li VHF radar: Technical layout and a summary of initial results, Radio Sci., 25(4), 487–502, doi:10.1029/RS025i004p00487, 1990.

Rüster, R., Klostermeyer, J. and Röttger, J.: SOUSY VHF Radar Measurements in the Lower and Middle Atmosphere, IEEE Transactions on Geoscience and Remote Sensing, GE-24, 6, 966-974, 1986.

Scargle, J. D.: Studies in astronomical time series analysis, I – Modeling random process in the time domain, Astrophysical J. Supplement Series, 45, 1–71, 1981.

Scargle, J. D.: Studies in astronomical time series analysis, II – Statistical aspects of spectral analysis of unevenly spaced data, Astrophysical J., 263, 835–853, 1982.

Selkirk, H. B.: The tropopause cold trap in the Australian monsoon during STEP/AMEX 1987. J. Geophys. Res. 98, 8591–8610, 1993.

Stober, G., Latteck, R., Rapp, M., Singer, W., and Zecha, M.: MAARSY – the new MST radar on Andøya: first results of spaced antenna and Doppler measurements of atmospheric winds in the troposphere and mesosphere using a partial array, Adv. Radio Sci., 10, 291-298, doi:10.5194/ars-10-291-2012, 2012.

Stober, G., Sommer, S., Rapp, M., and Latteck, R.: Investigation of gravity waves using horizontally resolved radial velocity measurements, Atmos. Meas. Tech., 6, 2893-2905, doi:10.5194/amt-6-2893-2013, 2013.

Tsuda, T., Sato, T., Hirose, K., Fukao, S., and Kato, S.: MU radar observations of the aspect sensitivity of backscattered VHF echo power in the troposphere and lower stratosphere, Radio Sci., 21(6), 971–980, doi:10.1029/RS021i006p00971, 1986.

Tsuda, T., Kato, S., Yokoi, T., Inoue, T., Yamamoto, M., VanZandt, T. E., Fukao, S., and Sato, T.: Gravity waves in the mesosphere observed with the middle and upper atmosphere radar, Radio Sci., 25(5), 1005–1018, doi: 10.1029/RS025i005p01005, 1990.

Tsuda, T., VanZandt, T. E., and Saito H.: Zenith-angle dependence of VHF specular reflection echoes in the lower atmosphere, J. Atmos. Sol. Terr. Phys., 59, 761–775, 1997.

Vincent, R. A., Kovalam, S., Fritts, D. C., and Isler, J. R.: Longterm MF radar observations of solar tides in the low-latitude mesosphere: Interannual variability and comparisons with the GSWM, J. Geophys. Res., 103, 8667–8683, 1998.

Waldteufel, P. and Corbin, H.: On the Analysis of Single-Doppler Radar Data, J. Appl. Meteorol., 18, 532–542, 1979.

Wang, C.: New Chains of Space Weather Monitoring Stations in China. Space Weather, 8: n/a. doi: 10.1029/2010SW000603, 2010.

Woodman, R. F., and Guille, A.: Radar Observations of Winds and Turbulence in the Stratosphere and Mesosphere, J. Atmos. Sci., 31, 493–505, 1974.

Woodman, R. F., and Chu, Y.-H.: Aspect sensitivity measurements of VHF backscatter made with the Chung-Li radar: Plausible mechanisms, Radio Sci., 24(2), 113–125, doi:10.1029/RS024i002p00113, 1989.

World Meteorological Organization (WMO): Measurements of upper air temperature, pressure, and humidity, in Guide to Meteorological Instruments and Methods of Observation, 6th ed., WMO I.12–1–I.12–32, Geneva, 1996.

Yamamoto, M., Fukao, S., Woodman, R. F., Ogawa, T., Tsuda, T., and Kato, S.: Mid-Latitude E Region Field-Aligned Irregularities Observed With the MU Radar, J. Geophys. Res., 96(A9), 15,943–15,949, 1991.

Yamamoto, M. K., M. Oyamatsu, T. Horinouchi, H. Hashiguchi, and S. Fukao, High time resolution determination of the tropical tropopause by the Equatorial Atmosphere Radar, Geophys. Res. Lett., 30(21), 2094, 2003.

Yang, P., Lu, D., Li, W., Wu, B., Fukao, S., Yamamoto, M., Tsuda, T., and Kato, S.: Chaotic features of the atmospheric motions near the tropopause revealed by MU radar observation: Case study, Radio Sci., 25(5), 1065–1070, 1990.

Zhang S. D. and Yi, F.: A statistical study of gravity waves from radiosonde observations at Wuhan (30°N, 114°E), China. Annales, Geophysicae, 23, 665-673, 2005.

Zhao Z. Y., Zhou, C., Qing, H. Y., Yang, G. B., Zhang, Y. N., Chen, G., Hu, Y. G.: Wuhan Atmosphere Radio Exploration (WARE) Radar: System Design and On-Line Winds Measurements, Radio Sci., 48, 326–333, 2013.

Zink, F., Vincent, R. A., Murphy, E., and Cote, O.: Comparison of radar and in situ measurements of atmospheric turbulence, J. Geophys. Res., 109, D11108, 2004.

Table 1. WAER Radar Technical Parameter

Aspect	Specifications
Radar system	
Operating Frequency	53.8MHz (=5.576m)
Power Synthesis	All solid state, Fully distributed
Peak Power	~172kW
Duty Cycle	Low mode 10%
	Medium mode 20%
	High mode 20%
Antenna system	
Antenna Array	24×24,active phased array
Antenna Type	Yagi aerial, 3 units, horizontal polarization
Normal Beam Width	≤4.5°half-power width, pencil beam
Voltage Standing Wave Ratio	≤1.1
Beam Direction	Five beams: vertical, off-zenith 0°- 20°by 1°
Antenna Operation Mode	Doppler Beam Swinging (DBS)
Experimental Specifications	
Pulse Width	1 μs (Low mode)
	32 μs (Medium mode)
	128 μs (High mode)
Interpulse Period (IPP)	160 μs (Low mode)
	320 μs (Medium mode)
	1280 μs (High mode)
No. of Coherent Integration	128 (Low mode)
	64 (Medium mode)
	8 (High mode)
No. of Incoherent Integration	10 (All modes)
No. FFT Points	256 (Low mode)
	256 (Medium mode)
	512 (High mode)
Time Resolution	1 minute

Figure Captions

Figure 1. (a) Power spectrum of four oblique beams. **(b)** Comparison of wind field observations between MST radar and rawinsonde for the altitude range of 3.2 to 16.9 km at 16:00 LT on September 11, 2011: (left) wind speed and (right) wind direction.

Figure 2. WARE observation of vertical wind velocity for 24 hours on October 2, 2012.

Figure ~~2~~3. WARE observations of mesospheric wind: (a) the spectrum power of four oblique beams, and (b) the meridional and zonal wind estimated from 69 to 85 km.

Figure ~~3~~4. (a) C_n^2 profile (green line) estimated by radar echo power and temperature profile (blue line) estimated by rawinsonde. **(b)** WARE observations of the radar echo power from 3.2 km to 16.9 km for continuous 20 hours. The black dotted line denotes the height of radar tropopause.

Figure ~~4~~5. Vertical profiles of (a) meridional, (c) zonal and (e) vertical wind disturbance components of the QM IGW observed at 06:05 LT on September 26, 2011. (g) is the hodograph of the fitted meridional wind versus zonal wind. (b), (d), (f) and (h) are the same as (a), (c), (e) and (g), while the time is 13:05 LT on September 26, 2011.

Figure ~~5~~6. Observations of the variation of echo power as a function of beam zenith angle at six specified heights at 4.75 km, 6.09 km, 9.13 km, 13.13 km, 15.24 km and 17.85 km by low and medium mode of WARE radar.

Figure ~~6~~ 7 (a) The raw time series for the meridional wind observed by WARE radar from October 1 to October 12, 2011, with height resolution of 0.15 km and temporal resolution of 30 minutes. **(b)** Lomb-Scargle periodogram meridional wind disturbances. Only the values with confidence levels greater than 95% are shown.

Figure ~~7~~ 8. Similar to Fig. 6, but for the zonal wind.

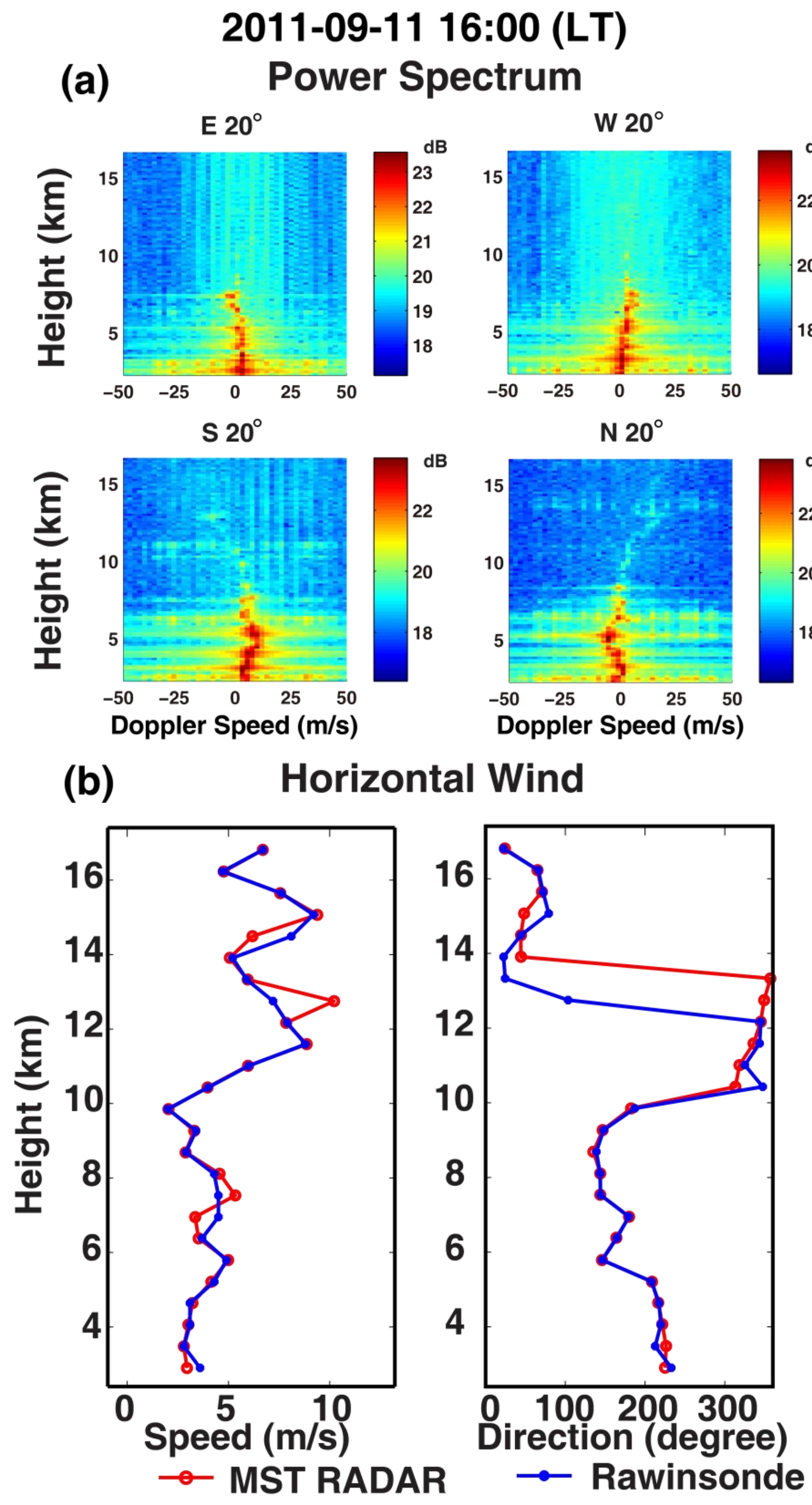

Figure 1. (a) Power spectrum of four oblique beams. **(b)** Comparison of wind field observations between MST radar and rawinsonde for the altitude range of 3.2 to 16.9 km at 16:00 LT on September 11, 2011: (left) wind speed and (right) wind direction.

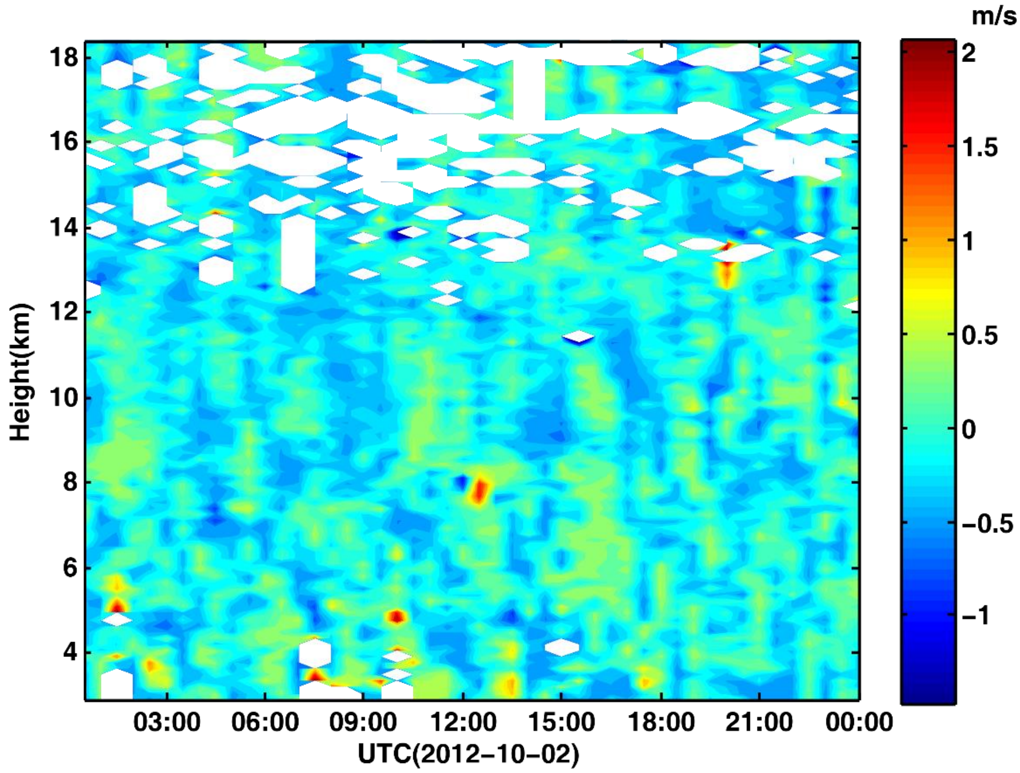

Figure 2. WARE observation of vertical wind velocity for 24 hours on October 2, 2012.

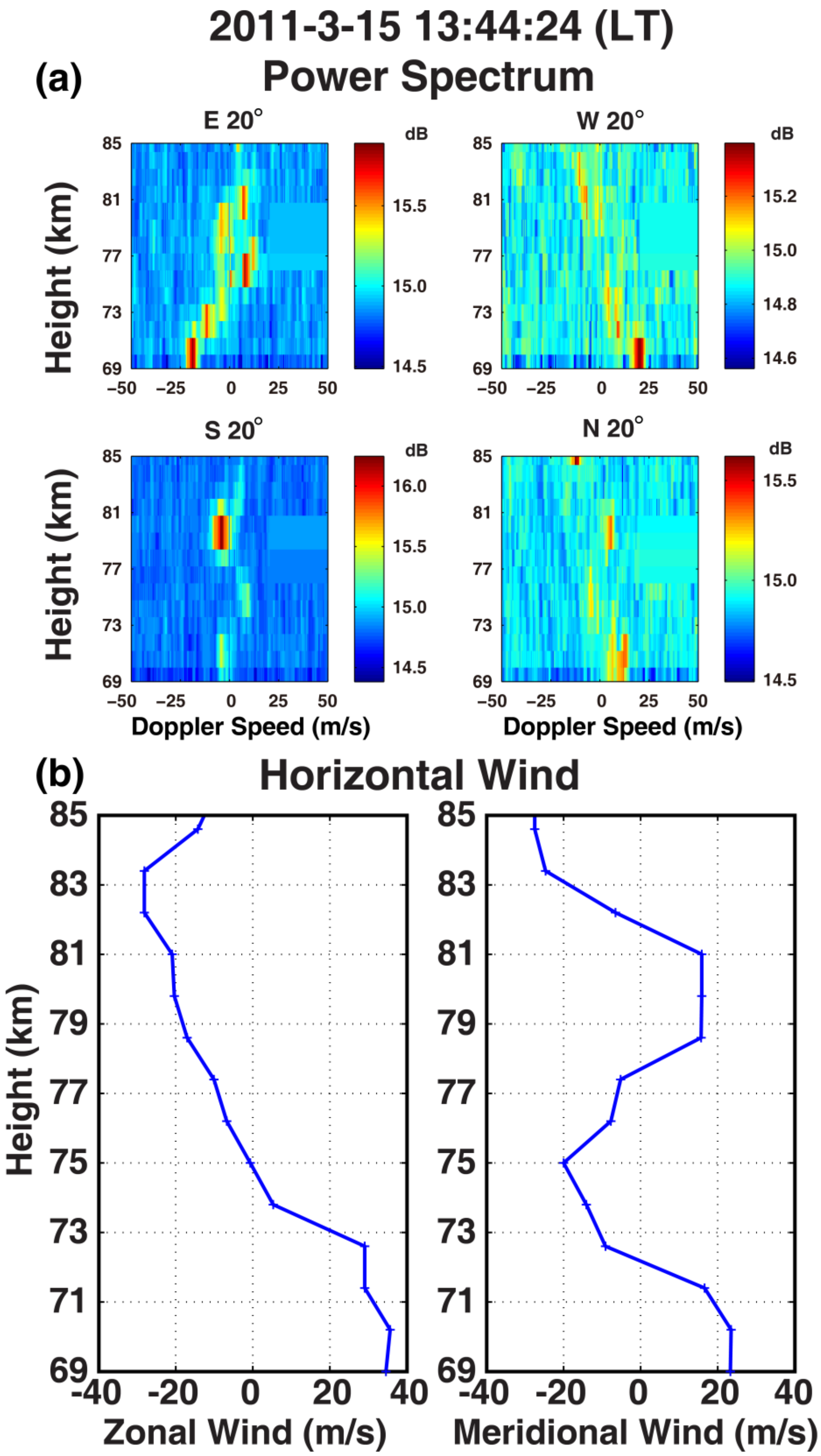

Figure ~~2~~3. WARE observations of mesospheric wind: (a) the spectrum power of four beams, and (b) the meridional and zonal wind estimated from 69 to 85 km.

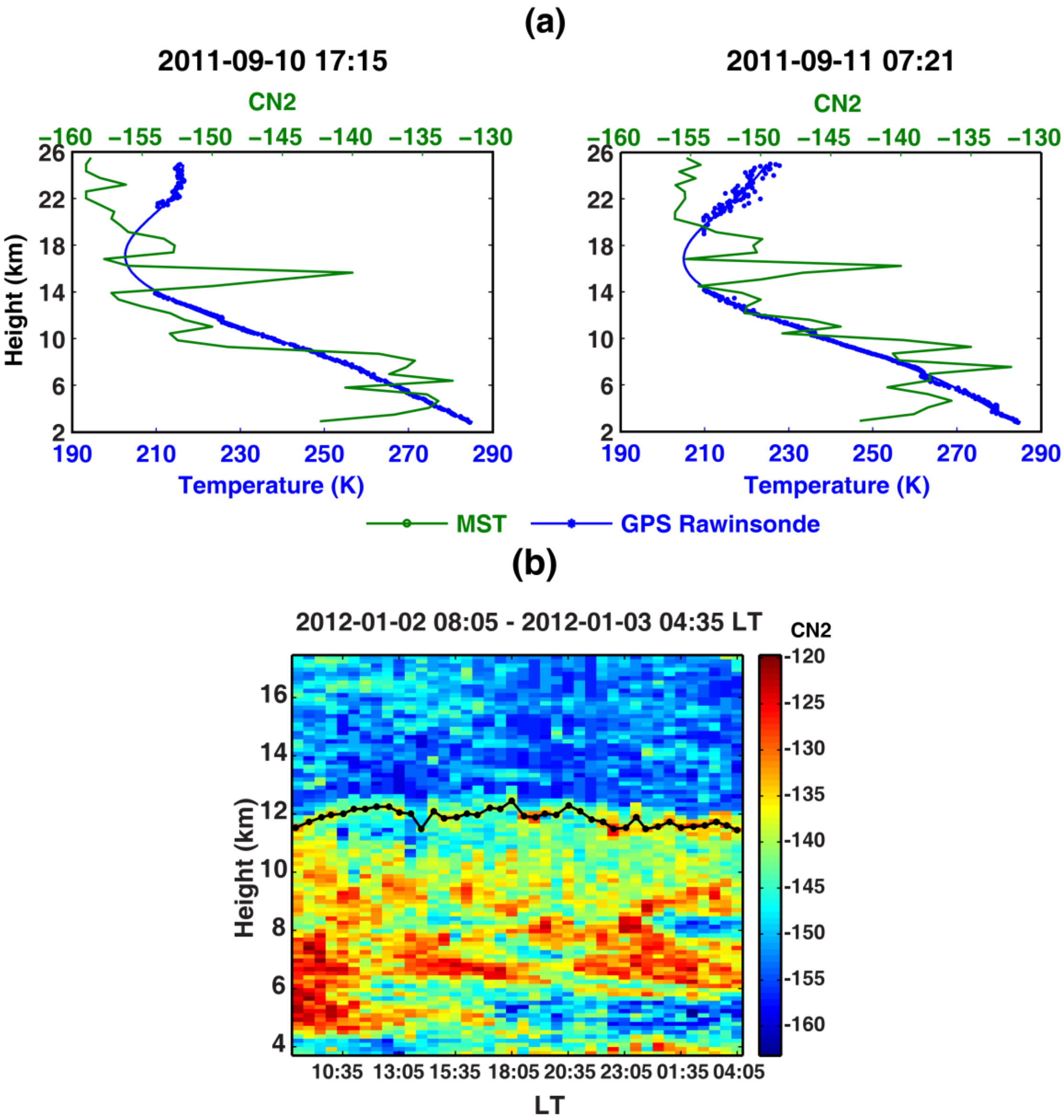

Figure ~~3~~4. **(a)** C_n^2 profile (green line) estimated by radar echo power and temperature profile (blue line) estimated by rawinsonde. **(b)** WARE observations of the radar echo power from 3.2 km to 16.9 km for continuous 20 hours. The black dotted line denotes the height of radar tropopause.

Figure 4

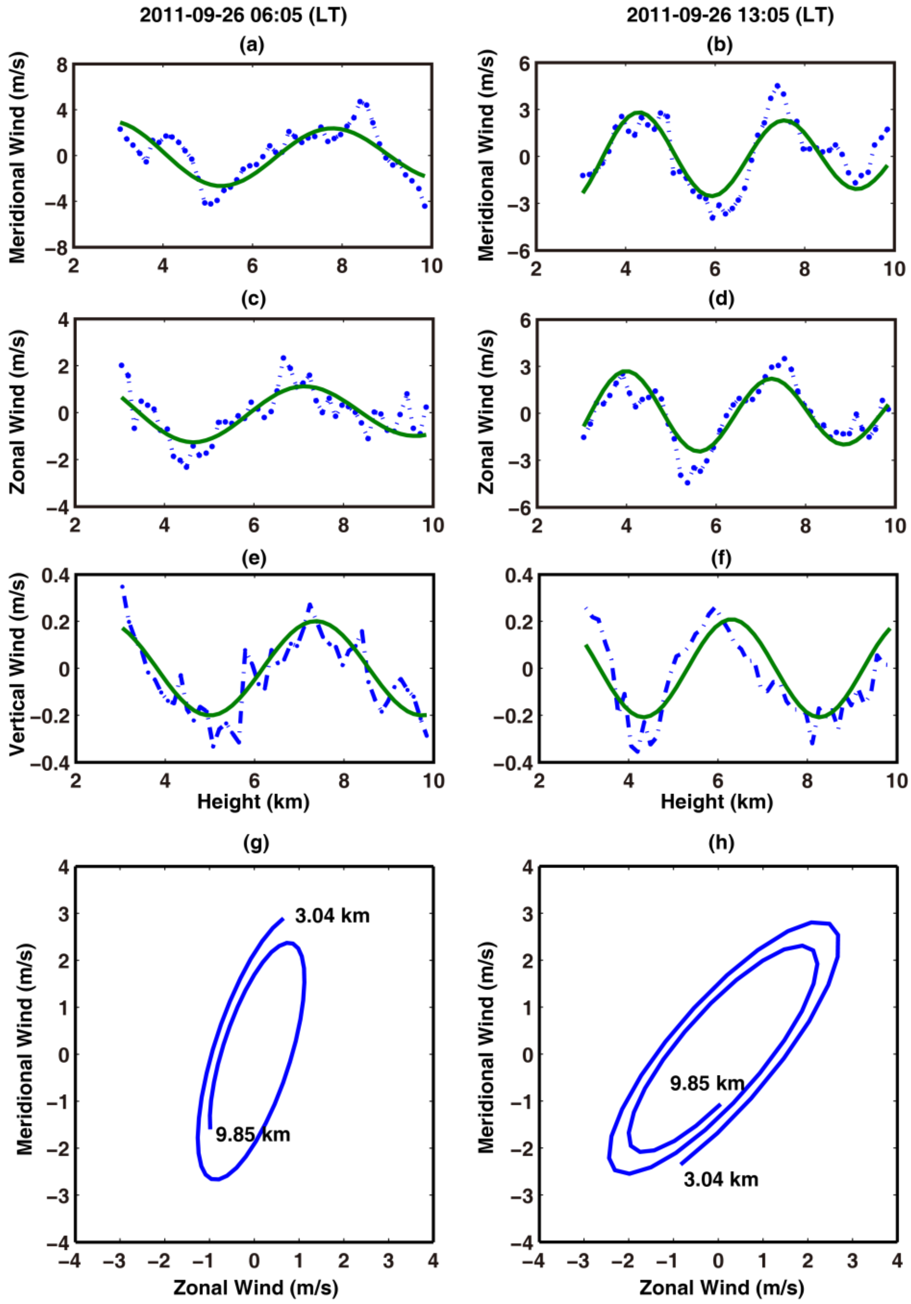

Figure 45. Vertical profiles of (a) meridional, (c) zonal and (e) vertical wind disturbance components of the QM IGW observed at 06:05 LT on September 26, 2011. (g) is the hodograph of the fitted meridional wind versus zonal wind. (b), (d), (f) and (h) are the same as (a), (c), (e) and (g), while the time is 13:05 LT on September 26, 2011.

Figure 5

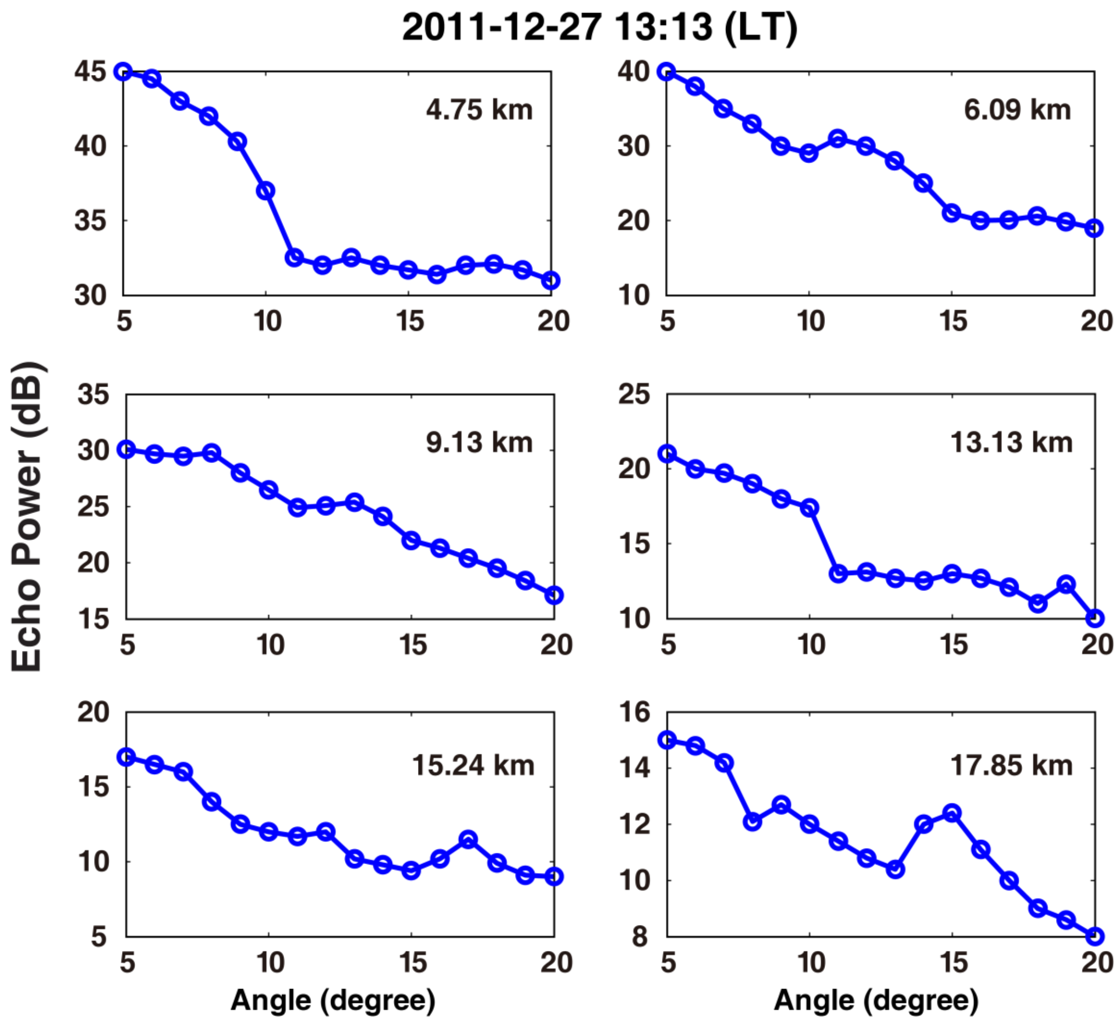

Figure ~~5~~6. Observations of the variation of echo power as a function of beam zenith angle at six specified heights at 4.75 km, 6.09 km, 9.13 km, 13.13 km, 15.24 km and 17.85 km by low and medium mode of WARE radar.

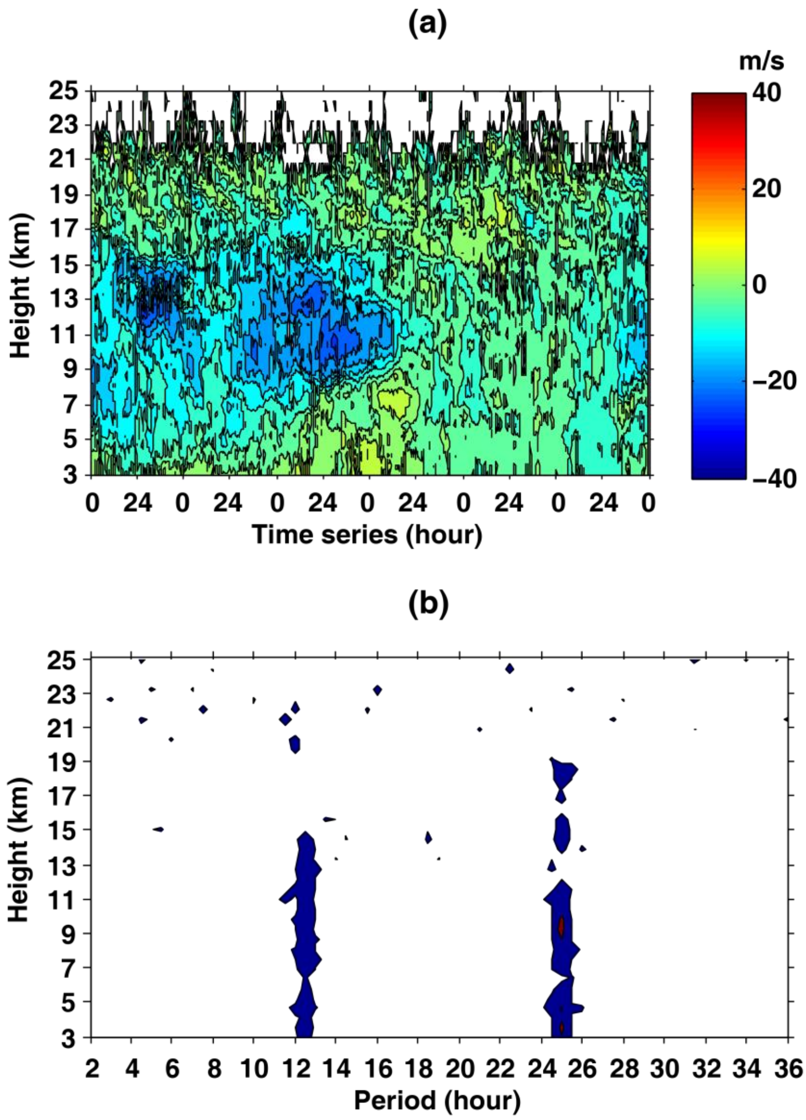

Figure ~~6~~ 7 (a) The raw time series for the meridional wind observed by WARE radar from October 1 to October 12, 2011, with height resolution of 0.15 km and temporal resolution of 30 minutes. **(b)** Lomb-Scargle periodogram of meridional wind disturbances. Only the values with confidence levels greater than 95% are shown.

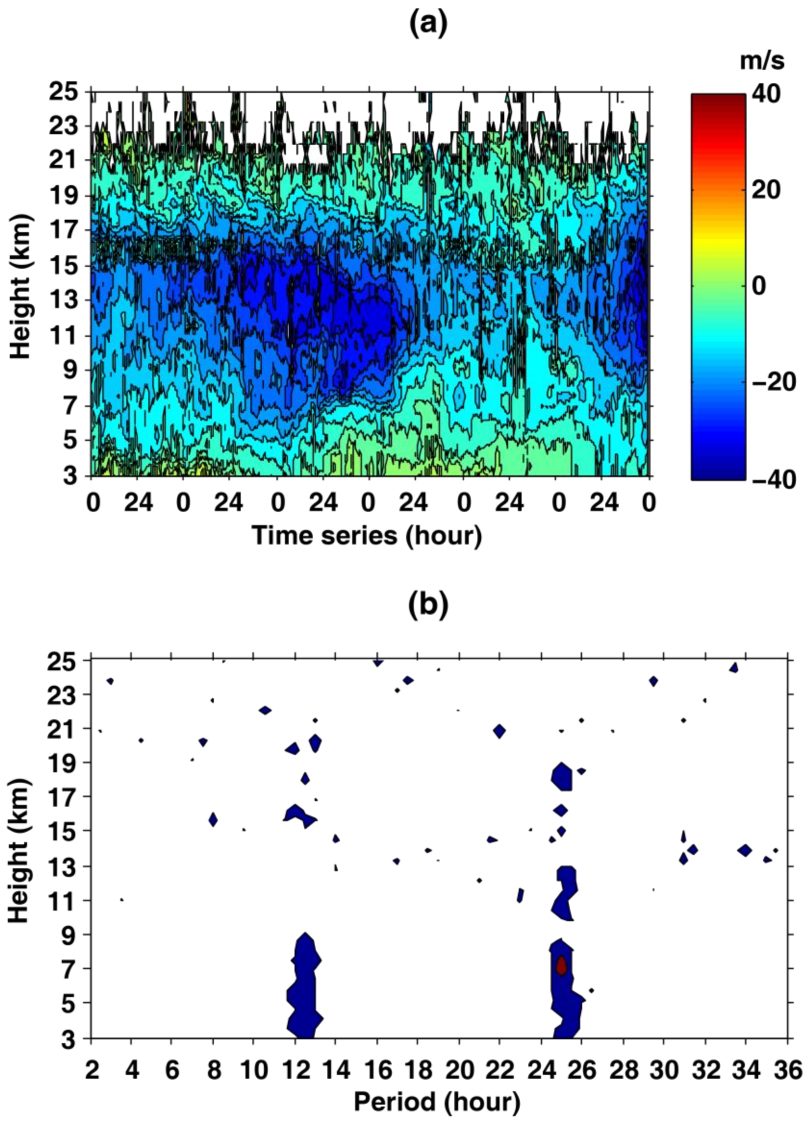

Figure ~~7~~8. Similar to Fig. 6, but for the zonal wind.